Patel, D. J., & Shapiro, L. (1986) *J. Biol. Chem. 261*, 1230-1239.
Pelton, J. G., & Wemmer, D. E. (1989) *Proc. Natl. Acad. Sci. U.S.A. 86*, 5723-5727.
Pelton, J. G., & Wemmer, D. E. (1990) *J. Am. Chem. Soc. 112*, 1393-1399.
Pjura, P. E., Grzeskowiak, K., & Dickerson, R. E. (1987) *J. Mol. Biol. 197*, 257-271.
Plateau, P., & Guéron, M. (1982) *J. Am. Chem. Soc. 104*, 7310-7311.
Portugal, J., & Waring, M. J. (1988) *Biochim. Biophys. Acta 949*, 158-168.
Rance, M., Sørensen, O. W., Bodenhausen, G., Wagner, G., Ernst, R. R., & Wüthrich, K. (1983) *Biochem. Biophys. Res. Commun. 117*, 479-485.
Scheek, R. M., Russo, N., Boelens, R., Kaptein, R., & van Boom, J. H. (1983) *J. Am. Chem. Soc. 105*, 2914-2916.
Scheek, R. M., Boelens, R., Russo, N., van Boom, J. H., & Kaptein, R. (1984) *Biochemistry 23*, 1371-1376.
Searle, M. S., & Embrey, K. J. (1990) *Nucleic Acids Res. 18*, 3753-3762.
Sinha, N. D., Biernat, J., McManus, J., & Köster, H. (1984) *Nucleic Acids Res. 12*, 4539-4557.
Steiner, R. F., & Sternberg, H. (1979) *Arch. Biochem. Biophys. 197*, 580-588.
Stevens, E. S., Sugawara, N., Bonora, G. M., & Toniolo, C. (1980) *J. Am. Chem. Soc. 102*, 7048-7050.
Stokke, T., & Steen, H. B. (1985) *J. Histochem. Cytochem. 33*, 333-338.
Sutherland, I. O. (1971) *The Investigation of the Kinetics of Conformational Changes by Nuclear Magnetic Resonance Spectroscopy*, Academic Press, London and New York.
Teng, M.-K., Usman, N., Frederick, C. A., & Wang, A. H. J. (1988) *Nucleic Acids Res. 16*, 2671.
Van de Ven, F. J. M., & Hilbers, C. W. (1988) *Eur. J. Biochem. 178*, 1-38.
Wüthrich, K. (1976) *NMR in Biological Research: Peptides and Proteins*, North-Holland Publishing Co., Amsterdam and Oxford.
Wüthrich, K. (1986) *NMR of Proteins and Nucleic Acids*, John Wiley & Sons, New York.
Zhang, X., & Patel, D. J. (1990) *Biochemistry 29*, 9451-9466.

Structure of the Pure-Spermine Form of Z-DNA (Magnesium Free) at 1-Å Resolution†,‡

Martin Egli,* Loren Dean Williams, Qi Gao,§ and Alexander Rich*
Department of Biology, Massachusetts Institute of Technology, Cambridge, Massachusetts 02139
Received August 5, 1991; Revised Manuscript Received September 11, 1991

ABSTRACT: We describe the three-dimensional X-ray structure of a complex of spermine bound to a Z-DNA duplex, $[d(CGCGCG)]_2$, in the absence of any inorganic polyvalent cations. We have crystallized the DNA hexamer d(CGCGCG) in the exclusion of magnesium and other polyvalent ions and solved its structure at 1.0-Å resolution. In the crystal of this pure-spermine form of Z-DNA, the relative orientation, position, and interactions of the DNA differ from the arrangement uniformly observed in over a dozen previously reported Z-DNA hexamers. Moreover, the conformation of the Z-DNA hexamer in this structure varies somewhat from those found in earlier structures. The DNA is compressed along the helical axis, the base pairs are shifted into the major groove, and the minor groove is more narrow. The packing of spermine–DNA complexes in crystals suggests that the molecular basis for the tendency of spermine to stabilize compact DNA structures derives from the capacity of spermine to interact simultaneously with several duplexes. This capacity is maximized by both the polymorphic nature and the length of the spermine cation. The length and flexibility of spermine and the dispersion of charge–charge, hydrogen-bonding, and hydrophobic bonding potential throughout the molecule maximize the ability of spermine to interact simultaneously with different DNA molecules.

Condensation of DNA into compact structures is cation dependent. The focus of this report is spermine, a member of a complex and nearly ubiquitous family of biological cations known as the polyamines [for reviews, see Morris (1981), Pegg and McCann (1982), Tabor and Tabor (1984), and Feuerstein et al. (1991)]. Spermine is the largest polyamine found in eukaryotes and, with a positive charge of 4 at pH 7, also the most highly charged. A series of larger polyamines (pentamines and hexamines) have been isolated from thermophilic bacteria. Spermine stabilizes duplex DNA against thermal denaturation (Mandel, 1962; Tabor, 1962; Bloomfield & Wilson, 1981; Thomas & Bloomfield, 1984) and can condense DNA (Gosule & Schellman, 1978; Chattoraj et al., 1978; Wilson & Bloomfield, 1979; Widom & Baldwin, 1980) and chromatin (Sen & Crothers, 1986) into compact structures.

We describe the three-dimensional X-ray structure of a complex of spermine bound to a Z-DNA duplex. Z-DNA was first detected with CD spectroscopy (Pohl & Jovin, 1972), and the three-dimensional structure of the Z conformation of [d-

† This research was supported by grants from the National Institutes of Health, the American Cancer Society, the National Science Foundation, the Office of Naval Research, and the National Aeronautics and Space Administration. M.E. acknowledges fellowship support by the Geigy-Jubiläums-Stiftung. L.D.W. acknowledges fellowship support by the National Institutes of Health and the Medical Foundation, Boston, MA.
* To whom correspondence should be addressed.
‡ The atomic coordinates have been deposited with the Brookhaven Protein Data Bank (entry number 1D48).
§ Current address: Analytical Research Department, Bristol Myers-Squibb, Wallingford, CT 06492.

0006-2960/91/0430-11388$02.50/0

Table I: Cell Constants of Selected Z-DNA Hexamers[a]

sequence	space group	a (Å)	b (Å)	c (Å)	remarks	ref
d(CGCGCG)	$P2_12_12_1$	17.88	31.55	44.58	Mg^{2+}/PA 3.4.3	Wang et al. (1979, 1981)
d(CGCGCG)	$P2_12_12_1$	18.01	31.03	44.80	Mg^{2+}	Gessner et al. (1989)
d(CGCGCG)	$P2_12_12_1$	18.00	30.96	44.83	Co^{3+}/Mg^{2+}	Gessner et al. (1985)
d(CGCGCG)	$P2_12_12_1$	18.06	30.95	44.98	Ru^{3+}	Ho et al. (1987)
d(*CG*CG*CG)	$P2_12_12_1$	17.76	30.57	45.42	* = m^5C/Mg^{2+}/PA3.4.3	Fujii et al. (1982)
d(*CG*CG*CG)	$P2_12_12_1$	18.01	30.88	44.76	* = Br^5C/Na^+	Westhof et al. (1985); Chevrier et al. (1986)
d(CGCGCG)	$P2_12_12_1$	17.94	31.23	44.55	Mg^{2+}/PA 2.4	Tomita et al. (1989)
d(CGCGCG)	$P2_12_12_1$	17.93	31.23	44.64	Mg^{2+}/PA 3.4	Tomita et al. (1989)
d(CGCGCG)	$P2_12_12_1$	17.98	31.51	44.38	Mg^{2+}/PA 3.3.4	Tomita et al. (1989)
d(CGCGCG)	$P2_12_12_1$	17.93	31.36	44.62	Mg^{2+}/PA 2.2.2	Tomita et al. (1989)
av cell constants		17.95	31.13	44.76		
d(CGCGCG)	$P2_12_12_1$	18.41	30.77	43.15	PA 3.4.3	this work

[a] Cations which were used for crystallization and found in the crystal lattice are listed under remarks. Polyamines (PA) are designated by three numbers indicating the length of the carbon chains between nitrogen atoms. Thus, PA 3.4.3 is spermine, PA 3.4 is spermidine, and PA 3.3.4 is thermospermine.

$(CGCGCG)]_2$ was later solved to atomic resolution by X-ray crystallography (Wang et al., 1979). B-DNA is most easily converted to Z-DNA in alternating pyrimidine–purine sequences (Rich et al., 1984) and is stabilized by high sodium (Pohl & Jovin, 1972) and magnesium concentrations (Chen et al., 1984), bromination (Möller et al., 1984) or methylation at the 5-position of cytosine (Behe & Felsenfeld, 1981), negative supercoiling (Peck et al., 1982; Singleton et al., 1982), and polyamines (Behe & Felsenfeld, 1981; Chen et al., 1984; Rao et al., 1990). Z-DNA crystals, in optimum cases, diffract X-rays to 1-Å resolution such that all atoms, including many water molecules and ions, are clearly visualized. The high resolution of Z-DNA crystal structures provides a wealth of information on the details of nucleic acid structure and interactions which generally cannot be obtained from crystal structures of A- or B-DNA.

Previous reports have described atomic resolution crystal structures of the Z conformation of $[d(CGCGCG)]_2$ in the presence of inorganic polyvalent cations. The "spermine form" (Wang et al., 1979), actually a "mixed magnesium/spermine form", contains one bound magnesium ion and two bound spermine molecules, whereas the "magnesium form" (Gessner et al., 1989) contains four magnesium ions bound to each hexamer duplex. The crystal structures of over a dozen additional Z-DNA hexamers, with varying sequences and modifications but always in the presence of inorganic cations (magnesium, cobalt, etc.), have been determined (see references in Table I). The orientation and position of the DNA is the same in all these crystals, and we will refer to this arrangement as the "magnesium" Z-DNA lattice. As described here, in the crystal of the pure-spermine form, which lacks magnesium or other bivalent or polyvalent cations, the relative orientation, position, and interactions of the DNA differ from the magnesium lattice. We will refer to this pure-spermine arrangement as the "spermine" Z-DNA lattice. Even though the pure-spermine lattice is different from the magnesium lattice, the crystallographic space group is maintained and the cell constants are altered only slightly. The effects of polyvalent ions appear to dominate the effects of spermine, as indicated by the previously described mixed spermine/magnesium form (Wang et al., 1979) which crystallized in the magnesium lattice.

NMR solution data previously suggested that the convex surface of Z-DNA is the favorable binding site for polyamines (Basu et al., 1988). Compared to solution techniques such as NMR, a fundamental disadvantage of the crystallographic approach is the requirement for the crystalline state. The conformation and interactions of DNA (or protein) in a crystal may differ from those in the solution state. However, tightly constrained DNA in chromatin, phage heads, and other compact structures is not "in solution". It would appear that DNA in such condensed states is well approximated by heavily hydrated crystalline states. Thus the "packing" of DNA into crystals can provide useful models for "packaging" of DNA in biological environments. As described in this report, the packing of spermine–DNA complexes in crystals suggests that the molecular basis for the tendency of spermine to stabilize compact DNA structures derives from the capacity of spermine to interact simultaneously with several duplexes. This capacity is maximized by both the polymorphic nature and the length of spermine. The length (15.4 Å from N1 to N14 in the pure-spermine form) and flexibility of spermine and the dispersion of charge–charge, hydrogen-bonding, and hydrophobic potential throughout the molecule maximizes its ability to interact simultaneously with different DNA molecules. Thus it is incorrect to consider spermine merely as four cationic charges covalently linked together.

Materials and Methods

DNA Synthesis and Purification. The self-complementary DNA hexamer d(CGCGCG) was prepared by the phosphotriester method on an ABI-380B DNA synthesizer. The deprotected oligomer was purified with preparative reverse-phase HPLC (RAININ Dynamax-300A, C_4-silica gel, 12-μm column). The buffer was 0.1 M triethylammonium acetate, pH 6.5, and a maximum concentration of 50% acetonitrile was used to elute the DNA.

Crystallization. Crystals were grown at room temperature in sitting drops using the vapor diffusion method. The crystallization mother liquor initially contained 1.4 mM DNA (single stranded), 20 mM sodium cacodylate buffer (pH 7), and 15 mM spermine tetrachloride. The sitting drops were equilibrated against a reservoir of 20% 2-methyl-2,4-pentanediol. After several weeks, crystals began to appear as rectangular plates. This crystal morphology is in contrast to the quasihexagonal shape of Z-DNA crystals containing polyvalent cations.

Data Collection and Reduction. A crystal with approximate dimensions 0.45 × 0.30 × 0.20 mm was sealed in a glass capillary with a droplet of mother liquor and mounted on a four-circle diffractometer (Rigaku AFC5R) equipped with a rotating copper anode and graphite monochromator ($\lambda_{CuK\alpha}$ = 1.5406 Å). The initial cell constants were calculated from 15 reflections with 2θ values between 4° and 8°. The cell was refined with 14 reflections in a 2θ range between 17° and 25°. The final cell constants were a = 18.405(2) Å, b = 30.768(3) Å, and c = 43.152(3) Å (the numbers in parentheses refer to the standard deviations of the last digit) and the space group

was determined as orthorhombic $P2_12_12_1$. A total of 17 410 reflections were measured at room temperature by the ω scan method (scan speed 4°/min.) to a resolution of 1 Å (2θ = 100°). Decay of the crystal was checked with three reflections with 2θ values between 25° and 55°. The maximum averaged decay after data collection was less than 8%. Data were corrected for Lorentz and polarization effects. A semiempirical absorption correction based on ψ scans for three reflections with χ values higher than 85° was applied (North et al., 1968). A total of 2500 reflections had been measured twice from two symmetry equivalent shells and merged with an R value of 2%. The number of unique reflections was 10 900 with 8200 reflections observed above the $2\sigma(F_{obs})$ level of which 2026 were between 1.2- and 1.0-Å resolution. This corresponds to 35% of the theoretically measurable reflections within that range.

Structure Solution and Refinement. As the space group was the same and the cell dimensions of the pure-spermine form crystals were similar to previously investigated crystals of Z-DNA hexamers, the structure was initially assumed to be isomorphous with the crystal structures of the other Z-DNA hexamers. Their cell constants together with those of the pure-spermine form described in this contribution are listed in Table I. The initial R factor obtained with a structure factor calculation using DNA coordinates from the $[d(CGCGCG)]_2$ mixed spermine/magnesium form crystal structure and 3-Å data (550 reflections) of the pure-spermine form was 59%, much higher than expected for two crystal structures with analogous orientations and positions of the DNA duplexes. However, Patterson maps revealed base stacking along the crystallographic c-axis. The helical axes were therefore expected to be roughly parallel to the c direction, as seen before with the Z-DNA hexamers. The correct orientation of the duplex was then determined using the molecular replacement method with the rotation/translation search program ULTIMA (Rabinovich & Shakked, 1984). The search revealed that the $[d(CGCGCG)]_2$ mixed spermine/magnesium form coordinates required a rotation around the c-axis (coinciding with the helical axis) and a shift along the c direction. The correct solution resulted in an R factor of 30%, using all 24 reflections within the resolution range between 25 and 9 Å. Including more data (251 reflections between 25 and 4 Å), as well as varying the two other rotational degrees of freedom and using smaller rotational and translational search grids, led to an R factor of 43% at this increased resolution, more than 5% lower than the second best solution. The final rotations indicated a slight tip of the helical axis with respect to the crystallographic c-axis. Figure 1 shows projections of the two distinct duplex orientations found with different crystal forms of $[d(CGCGCG)]_2$. A comparison of the duplex orientation in the pure-spermine form of $[d(CGCGCG)]_2$ (Figure 1A) with those in the magnesium or mixed spermine/magnesium forms (Figure 1C) shows a rotation around the c-axis by about 70°. At the same time, the duplex is shifted along the c-axis by about 2.9 Å or roughly by one base-pair step (Figure 1B). Whereas the angles between the helical axes and the c directions in the magnesium and mixed spermine/magnesium forms are 0.5° and 2.9°, respectively (Gessner et al., 1989), the duplex is slightly more inclined with respect to the c-axis in the pure-spermine crystal structure (3.4°).

The DNA positions and isotropic temperature factors were refined with 3-Å data using the Konnert–Hendrickson least-squares procedure (Hendrickson & Konnert, 1981) as modified for nucleic acids (Quigley et al., 1978) with relatively tight stereochemical constraints. As additional data were included, the structure factors were weighted more heavily. At an R factor of 32% (1.7-Å resolution, 2679 reflections), Fourier electron sum- ($2F_{obs} - F_{calc}$) and difference-density maps ($F_{obs} - F_{calc}$) were calculated and displayed on an Evans and Sutherland PS390 graphics terminal with the program FRODO (Jones, 1978). Correctly placed portions of a structure lie in electron sum density with no electron difference density present. Incorrectly placed portions of a structure result in the presence of both electron sum and difference densities, whereas missing portions result in areas of superimposed sum and difference densities. In the displayed electron-density

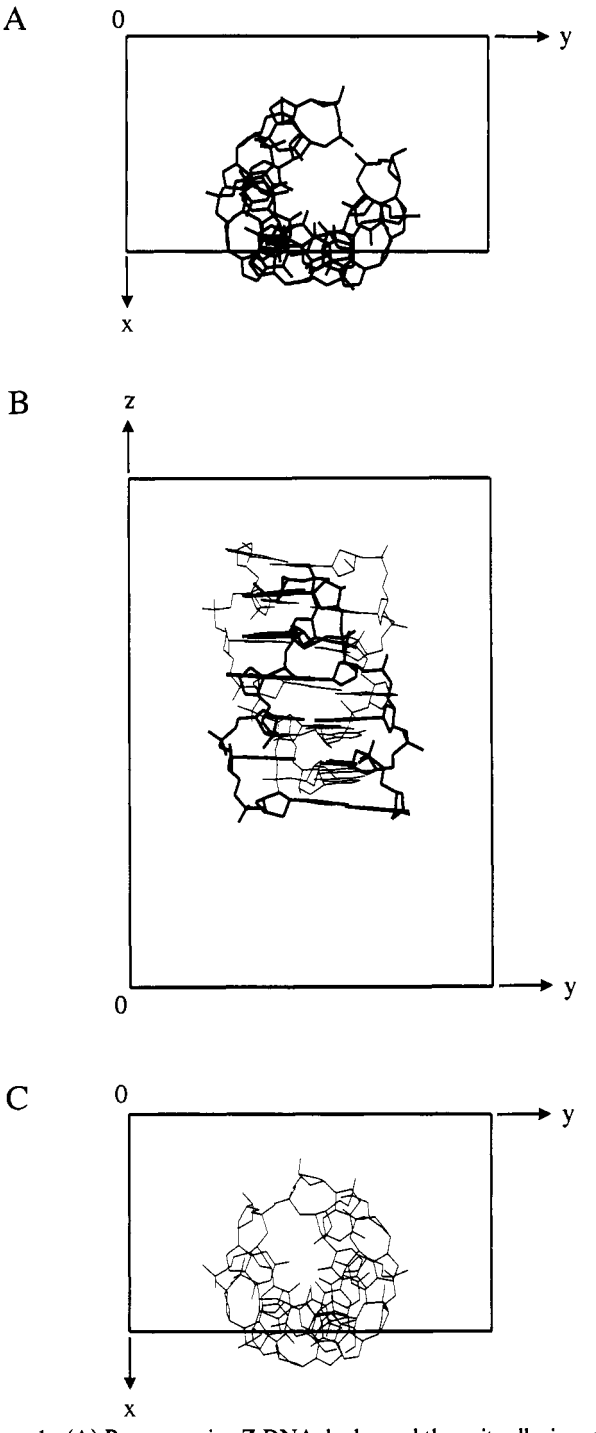

FIGURE 1: (A) Pure-spermine Z-DNA duplex and the unit cell, viewed along the z direction. (B) Superposition of the pure-spermine form (thick lines) with the mixed spermine/magnesium form (thin lines) within the unit cell of the pure-spermine form, viewed along the x direction. (C) For a comparison with panel A, the Z-DNA hexamer of the mixed spermine/magnesium (similar to the magnesium form) viewed along the z direction.

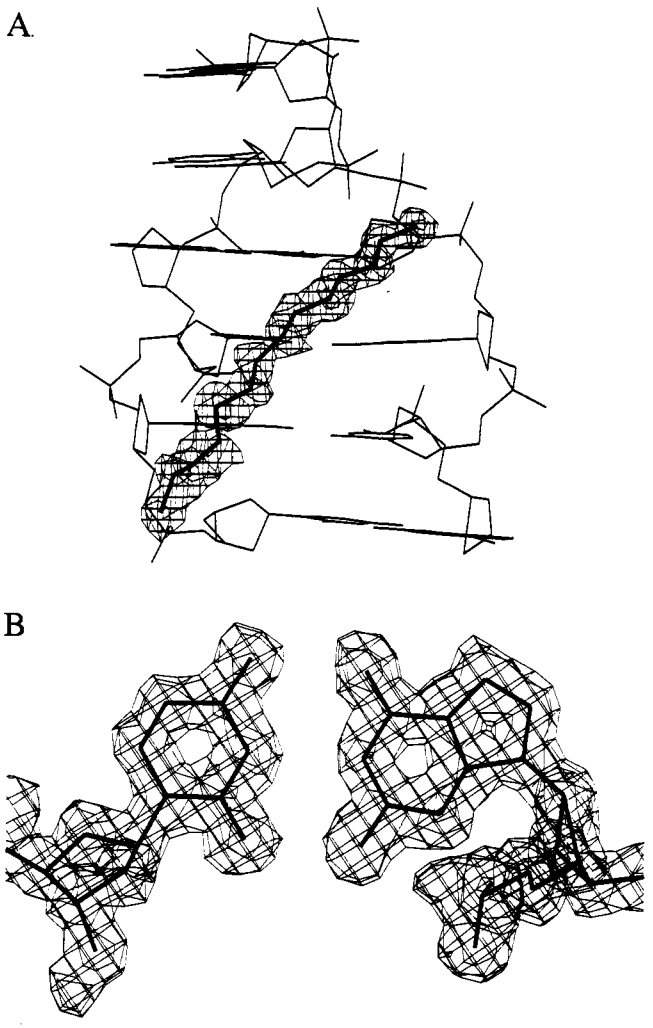

FIGURE 2: (A) Sum electron-density map ($2F_{obs} - F_{calc}$) around the spermine molecule (thick lines). The DNA is drawn with thin lines. (B) Sum electron-density map around the terminal base pair G(6)–C(7).

maps, a continuous band of sum and difference density was found and assigned to a spermine molecule. The positions of the spermine atoms were included in the refinement. At higher resolution, positions of water molecules were determined from sum and difference maps. For the final cycles of refinement, 8183 reflections at 1-Å resolution were included in the refinement, and, after relaxing the refinement constraints, the R factor converged at 18.5%. The asymmetric unit contained one DNA hexamer duplex, one spermine molecule, and 47 water molecules. Table II gives a list of selected refinement parameters. Figure 2A shows an electron-density sum map around the spermine molecule, and Figure 2B shows the electron-density sum map around the G(6)–C(7) base pair. Both maps were calculated at 1-Å resolution.

Results

DNA Conformation. The DNA in the pure-spermine lattice is rotated 70° around the helical axis, shifted by 3 Å in the direction of the helical axis, and rotated around the intramolecular pseudo-2-fold axis (perpendicular to the helical axis) compared to the DNA in the magnesium lattice (Figure 1). After simple superposition of the pure-spermine and mixed spermine/magnesium forms, the RMS deviation of atomic positions is 1.04 Å. This superposition was accomplished by a 70° rotation around the 2-fold screw axis running along the c direction and a 3 Å shift in the c direction (as described in the Materials and Methods). However, after also rotating the pure-spermine form duplex around the intramolecular pseudo-2-fold axis, and superimposing the G(6)–C(7) base pair of one duplex on the C(1)–G(2) base pair of the other, the RMS deviation of atomic positions is less, 0.34 Å. The C(1) → G(6) strand (5′ to 3′ direction) of the hexamer in the pure-spermine form is conformationally more similar to the C(7) → G(12) strands (5′ to 3′ direction) in the mixed spermine/magnesium and magnesium forms. The DNA atoms in the pure-spermine form have therefore been numbered such that atom O5′ of residue C(1) (e.g.) corresponds to atoms O5′ of residues C(7) in the mixed spermine/magnesium and magnesium forms.

In both lattices, the duplex contains a pseudo-2-fold axis. For the pure-spermine form the RMS deviation of atomic

Table II: Selected Crystallographic Refinement Parameters

parameters	values
total number of non-hydrogen atoms	301
DNA non-hydrogen atoms	240
cation and water non-hydrogen atoms	61
number of $F_{obs} > 2\sigma(F_{obs})$	8183
total number of variables [(number of atoms × 4) plus overall scale factor]	1205
overdeterminancy ratio (F_{obs}/variables)	6.8
total number of restraints (bond lengths, bond angles, planar groups, chiral volumes, van der Waals contacts)	1957
data-to-restraint ratio	4.2
final R factor (%)	18.5
R factors within shells (%)	
10.0–5.0 Å	18.5
5.0–3.0 Å	11.5
3.0–2.5 Å	16.5
2.5–2.0 Å	15.6
2.0–1.7 Å	15.7
1.7–1.5 Å	17.2
1.5–1.2 Å	23.4
1.2–1.0 Å	31.8
final weight (w^a) on structure factors	10.0
final fractional mean shifts for positions	<0.001
final mean shifts for B factors	<0.01
av $\lvert F_{obs} - F_{calc}\rvert$ for all reflections	9.2
av $\lvert F_{obs} - F_{calc}\rvert$ as a function of shells and number of contributing reflections in parentheses	
10.0–5.0 Å	29.3 (117)
5.0–3.0 Å	18.7 (435)
3.0–2.5 Å	15.7 (398)
2.5–2.0 Å	11.5 (825)
2.0–1.7 Å	9.0 (1006)
1.7–1.5 Å	7.4 (1047)
1.5–1.2 Å	7.0 (2328)
1.2–1.0 Å	7.5 (2027)
RMS deviations from *ideal* distances (Å) (Hendrickson & Konnert, 1981)	
single bond lengths	0.029
single bond angles	0.039
double bond lengths	0.016
double bond angles	0.036
hydrogen bond lengths	0.041
RMS deviations from planes (Å)	0.018
RMS deviations of chiral volumes (Å^3)	0.166
RMS deviations from minimal van der Waals distances between atoms (Å)	
separated by two bonds	0.14
separated by more than two bonds or nonbonded	0.14

[a] The minimized weighted function Φ_F for structure factors is

$$\Phi_F = \sum_{i=1}^{n(obs)} (1/w)^2[|F_{obs}(i)| - |F_{calc}(i)|]^2$$

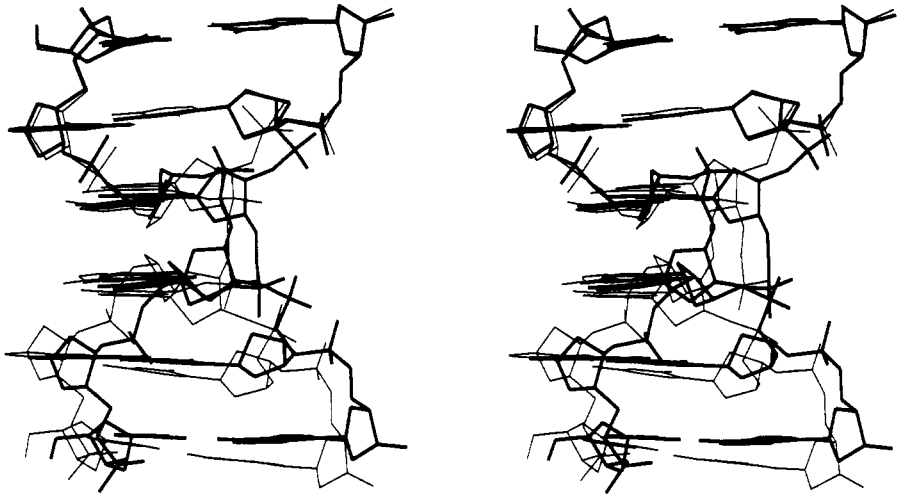

FIGURE 3: Comparison of the DNA conformations of the hexamer in the pure-spermine form (bold lines) and the hexamer in the magnesium form (thin lines). To emphasize the conformational deviations, the terminal residues [C(1)–G(12)] of the two structures were superimposed.

Table III: (A) Selected Helical Parameters and (B) Phosphate–Phosphate Distances for the Pure-Spermine Form, the Magnesium Form (Gessner et al., 1989) and the Mixed Spermine/Magnesium Form (Wang et al., 1979) of $[d(CGCGCG)]_2$[a]

A. Selected Helical Parameters[b]

pure-spermine form					magnesium form					mixed spermine/magnesium form				
incl	x_{dsp}	y_{dsp}	twist	rise	incl	x_{dsp}	y_{dsp}	twist	rise	incl	x_{dsp}	y_{dsp}	twist	rise
4.60	4.54	−2.46	10.89	3.70	6.93	3.29	−2.12	7.36	3.95	9.26	3.19	−2.40	7.59	4.07
5.62	4.26	1.80	50.89	3.66	6.06	3.35	2.21	50.68	3.65	8.44	3.12	1.87	50.22	3.68
6.24	3.41	−2.45	10.23	3.69	6.39	3.29	−2.16	7.77	3.98	8.64	3.04	−2.42	8.16	3.99
4.96	3.66	1.85	49.72	3.63	7.46	3.25	2.26	52.12	3.41	9.03	3.02	1.95	52.44	3.37
4.53	3.68	−2.67	9.85	3.66	6.87	3.31	−2.10	10.75	4.02	8.22	2.97	−2.25	9.74	4.33
5.35	3.27	1.84			7.17	3.17	2.16			9.84	2.63	1.68		
(5.22)	(3.80)	(−0.35)	(26.32)	(3.67)	(6.81)	(3.28)	(0.04)	(25.73)	(3.80)	(8.91)	(2.99)	(−0.26)	(25.63)	(3.89)

B. Intrastrand and Interstrand Phosphate–Phosphate Distances (Å)[c]

	pure-spermine form	magnesium form	mixed spermine/magnesium form
intrastrand			
P2–P4	10.29	9.97	10.31
P4–P6	8.87	9.35	8.77
P6–P2*	8.74	10.33	10.21
P8–P10	8.62	9.65	10.52
P10–P12	10.21	9.72	9.91
P12–P8*	8.63	9.83	9.22
	(9.23)	(9.81)	(9.82)
interstrand			
P2–P8*	8.58	8.56	8.53
P4–P12	8.37	8.79	8.64
P6–P10	8.43	8.57	8.88
P2–P10*	8.74	10.91	10.56
P4–P8*	10.30	11.59	11.12
P6–P12	10.56	11.00	11.50
	(9.16)	(9.90)	(9.87)

[a] The helical parameters were calculated with program NEWHELIX [version NEWHEL90 (Dickerson et al., 1989)]. [b] 5' to 3' direction; incl and twist are in degrees, and x_{dsp}, y_{dsp}, and rise are in angstroms; average values are given in parentheses. [c] Asterisks designate symmetry-equivalent atoms of adjacent duplexes; average values are given in parentheses.

positions of the two strands is 0.98 Å, and for the mixed spermine/magnesium and magnesium forms the RMS deviation of atomic positions of the two strands is 1.10 Å.

The DNA conformation, which is nearly invariant in the magnesium and mixed spermine/magnesium forms of $[d(CGCGCG)]_2$, differs significantly in the pure-spermine form. The RMS deviation of positions of DNA atoms of the magnesium and mixed spermine/magnesium forms is 0.20 Å. As described above, the RMS deviation of positions of DNA atoms of the pure-spermine and mixed spermine/magnesium forms is 0.34 Å.

Unlike an overall measure of similarity characterized by an RMS deviation, a partial superposition reveals distinct conformational alterations of the DNA in different crystal forms. The differences in conformation are most clearly revealed by superimposing the terminal base pairs of the different forms of $[d(CGCGCG)]_2$. This superposition is shown in Figure 3, and helical parameters as well as selected phosphate–phosphate distances of the three forms are listed in Table III. From Figure 3, it is evident that the duplex in the pure-spermine form is shorter than that in the magnesium form (and all the other Z-DNA hexamers crystallized thus far). The average helical rise of the DNA in the pure-spermine form is 3.67 Å. Thus, the rise in this form is 0.13 Å less than the average value in the magnesium form and is 0.22 Å less than the average value in the mixed spermine/magnesium form (see Table III, section A). The hexamer duplex in the pure-spermine form is thus 0.65 Å shorter than that of the magnesium form and

Table IV: DNA Backbone Torsion Angles, Glycosyl Torsion Angles χ, Pseudorotation Phase Angles P (in Degrees), and Sugar Puckers[a]

parameter	C(1)	G(2)	C(3)	G(4)	C(5)	G(6)	C(7)	G(8)	C(9)	G(10)	C(11)	G(12)
α		65	−150	59	−167	78		66	**−167***	69	−153	76
		2	6	11	2	4		5	**27**	5	5	2
		3	3	5	1	1		1	5	5	3	8
β		−174	−135	−165	**−141***	−180		−173	**−141***	180	**−137**	−172
		0	10	7	**26**	2		0	7	1	**13**	**4**
		2	14	9	**19**	5		2	**23**	5	**18**	5
γ	55	178	58	−176	54	−173	60	−177	59	177	52	−170
	8	4	8	2	11	7	7	2	4	2	2	4
	3	1	8	3	6	5	5	5	**4**	2	4	7
δ	140	98	148	92	133	149	139	101	142	97	139	143
	4	4	4	3	9	0	8	6	7	6	4	6
	5	7	0	0	9	0	0	0	2	1	3	6
ε	−91	−110	−90	**−128***	−94		−90	−114	−91	**−132**	−96	
	2	10	12	**51**	1		1	2	7	**20**	2	
	4	10	10	**51**	6		2	10	1	16	5	
ζ	75	−68	83	**−36***	65		72	**−47***	71	**−52**	69	
	6	2	7	**29**	9		6	**27**	9	**18**	3	
	4	3	2	**33**	15		2	**22**	3	**18**	1	
χ	−151	66	−163	55	−157	78	−161	59	−154	64	−162	74
	0	9	5	2	12	1	19	10	6	1	6	5
	1	6	13	4	5	0	10	2	0	2	6	1
P	152	22	158	37	141	170	152	34	150	28	151	164
	3	9	11	6	14	9	10	5	5	10	3	4
	2	17	12	11	10	0	4	2	3	7	0	2
pucker	C2′-endo	C3′-endo	C2′-endo	C4′-exo	C1′-exo	C2′-endo	C2′-endo	C3′-endo	C2′-endo	C3′-endo	C2′-endo	C2′-endo
	C2′-endo	C3′-endo	C2′-endo	C3′-endo	C2′-endo	C2′-endo	C2′-endo	C3′-endo	C2′-endo	C3′-endo	C2′-endo	C2′-endo
	C2′-endo	C4′-exo	C2′-endo	C3′-endo	C2′-endo	C2′-endo	C2′-endo	C4′-exo	C2′-endo	C3′-endo	C2′-endo	C2′-endo

[a] The three numbers per parameter are the actual value for the pure-spermine form (top) and the absolute differences to mixed magnesium/spermine form (middle) and magnesium form (bottom), respectively. The backbone torsion angles are defined as O3′–P–α–O5′–β–C5′–γ–C4′–δ–C3′–ε–O3′–ζ–P–O5′. Differences in backbone torsions due to the ZII conformation of P-5 and the partial ZII conformation of P-9 in mixed magnesium/spermine and magnesium form are in bold and marked with an asterisk. Other notable differences are in bold.

is 1.1 Å shorter than that of the mixed spermine/magnesium form.

A nominal complete turn of a Z-DNA helix (12 base pairs per turn) based on the average rise of the pure-spermine form would thus be 1.43 Å shorter than a complete turn based on the average rise of the magnesium form DNA. It would be 2.42 Å shorter than a complete turn based on the average rise of the mixed spermine/magnesium form DNA.

The DNA in the pure-spermine form displays values for the helical twist which are similar to those in the two other forms. The DNA in the pure-spermine form is slightly overwound in comparison with the magnesium and mixed spermine/magnesium forms. For the pure-spermine form, there are 5.98 repeats per turn (in Z-DNA, the repeat step consists of two residues). In the magnesium form, there are 6.04 repeats per turn, and, in the mixed spermine/magnesium form, there are 6.03 repeats per turn.

The largest difference between the helical parameters of the pure-spermine form and those in the magnesium lattice are found in the *x* displacement (x_{dsp}), the offset of the midpoint of the C6(pyrimidine)–C8(purine) line of a base pair from the helical axis (Dickerson, 1989). The base pairs in the pure-spermine form DNA have shifted outward into the major groove, away from the helical axis. The result of this x_{dsp} is that the helical axis of the pure-spermine form lies within the minor groove instead of passing through the O2 oxygens of cytosines. The difference between the average x_{dsp} of the pure-spermine form and the magnesium form is 0.52 Å, and the corresponding difference between the pure-spermine form and the mixed spermine/magnesium form is 0.81 Å (Table III, section A). The extent of x_{dsp} in the pure-spermine form varies from one base pair to the next. Therefore, the offsets between individual pairs of base pairs when going along the helix are uneven, resulting in different overlaps between stacked base pairs. In the magnesium form and the mixed spermine/magnesium forms, the x_{dsp} are more uniform. The variations of inclination between different base pairs are similar in the three forms. In the pure-spermine form, the mean inclination is 5.22°, and, in the magnesium and mixed spermine/magnesium forms, the mean inclinations are 6.81° and 8.91°, respectively (Table III, section A).

The compression of the helical axis and the generally more compact conformation of the DNA in the pure-spermine form is apparent from the phosphate–phosphate distances listed in Table III, section B. The average intrastrand phosphate–phosphate distances for the two strands in the pure-spermine form DNA are 0.58 Å shorter than the corresponding distances in the magnesium and mixed spermine/magnesium forms. Similarly, the distances between phosphates of different strands (interstrand distances) are generally shorter in case of the pure-spermine form DNA. The average distance in the pure-spermine form is 0.74 Å shorter than in the magnesium form, and it is 0.71 Å shorter than in the mixed spermine/magnesium form. Thus, the minor groove of the DNA in the pure-spermine form is more narrow than in the other forms.

Differences between the torsion angles of the DNA in the three forms are generally small (Table IV). However, certain torsion angles of the pure-spermine form are distinctly different from those of the mixed spermine/magnesium and magnesium forms. On one strand, these torsion angles are ε and ζ of residue G(4) and β of residue C(5). On the other strand, these torsion angles are ζ of residue G(8). Certain torsion angles of the mixed spermine/magnesium form differ from those of the magnesium form. In these cases, the pure-spermine form appears to adopt a hybrid conformation, intermediate between the other two forms. The α torsion angle of residue C(9) of

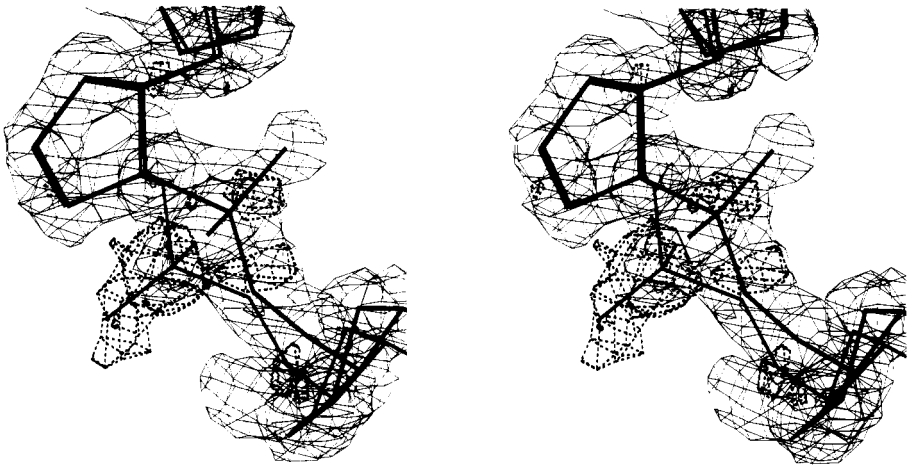

FIGURE 4: Backbone of residues G(8) and C(9) around phosphate P9 in the pure-spermine form in the ZI conformation (thick lines). The ZII conformation backbone of the magnesium form (thin lines) has been superimposed on the sugars of residues G(8) and C(9) of the pure-spermine form and fit into the difference density to illustrate the partial occupancy of the ZII conformation in the pure-spermine form at this site. Electron-density sum and difference ($F_{obs} - F_{calc}$) maps are represented as nets of thin lines (sum map) and thick dashed (difference map) lines.

the pure-spermine form is similar to that of the magnesium form but different from that of the mixed spermine/magnesium form. Conversely, the β torsion angle of the same residue is similar to the magnesium form but different from the mixed spermine/magnesium form.

The ZI and ZII conformations of Z-DNA (Wang et al., 1981) are distinguishable primarily by differences in the torsion angles ϵ and ζ and to a lesser degree by differences in α and β. The backbone torsion angles of the mixed spermine/magnesium and the magnesium forms are similar to each other in the region around the phosphate of residue C(5) but differ from the pure-spermine form (Table IV). In the mixed spermine/magnesium form, the backbone torsion angles around the phosphate of residue C(5) are ϵ[G(4)] = −179° (ap), ζ[G(4)] = 66° (+sc), α[C(5)] = 168° (ap), and β[C(5)] = 166° (ap) [the standard nomenclature of the ranges into which the torsion values fall is given in parentheses (Klyne & Prelog, 1960)]. In the magnesium form, the corresponding torsion angles are ϵ[G(4)] = −179° (ap), ζ[G(4)] = 69° (+sc), α[C(5)] = 166° (ap), and β[C(5)] = 160° (ap). In the pure spermine form, the corresponding torsion angles are ϵ[G(4)] = −128° (−ac), ζ[G(4)] = −36° (−sc), α[C(5)] = −167° (ap), and β[C(5)] = −141° (ap). The differences between the torsion angles of the pure-spermine form and mixed spermine/magnesium form (magnesium form in parentheses, note that Table IV lists the absolute differences) are $\Delta\epsilon$ = 51° (51°), $\Delta\zeta$ = 102° (105°), $\Delta\alpha$ = 25° (27°), and $\Delta\beta$ = 53° (59°).

The DNA backbone in the pure-spermine form is disordered in the region around the phosphate group of residue C(9). This disorder is shown in Figure 4. The backbone refines in a well-behaved way in the ZI conformation. However, both the sum and difference electron density (Figure 4) indicate that the ZII conformation is also partially occupied. This region of the backbone contains the predominant fraction of the total difference density of the asymmetric unit. The backbone around P5 of the magnesium form, which adopts the ZII conformation, is nearly superimposable on this string of difference density (Figure 4). In the mixed spermine/magnesium and magnesium forms, the backbone in the region around the phosphate of residue C(9) adopts a partial ZII conformation. The conformation of the pure-spermine form is more similar to the mixed spermine/magnesium and magnesium forms in the region of the backbone around the phosphate of residue C(9) than around the phosphate of residue C(5). For the four torsion angles involved in this conversion from ZI to partial ZII, the differences between pure-spermine form and mixed spermine/magnesium and magnesium forms (in parentheses) are $\Delta\epsilon$ = 2° (10°), $\Delta\zeta$ = 27° (22°), $\Delta\alpha$ = 27° (5°), and $\Delta\beta$ = 7° (23°). The differences are thus smaller, and the values of the torsion angles fall into the same conformational ranges in the three structures. The remaining differences in backbone torsion angles of the pure-spermine form in comparison with the mixed spermine/magnesium and magnesium forms, unlike the differences between the ZI and ZII conformations, do not alter torsion angles.

The glycosyl torsion angles and pseudorotation phase angles (Table IV) of the pure-spermine form are generally similar to those of the mixed spermine/magnesium and magnesium forms. Although the sugar puckers for residues G(4) and C(5) of the pure-spermine form fall into a different range than in the other two forms, the listed values for the phase angles show only small differences due to the conformational and energetic similarity of the C4′-*exo* and C3′-*endo* sugar conformations [G(4) residue] and the C1′-*exo* and C2′-*endo* sugar conformations, respectively [C(5) residue]. Moreover, similar differences with sugar puckers exist between the mixed spermine/magnesium and magnesium forms as well [residues G(2) and G(8), Table IV].

Spermine Conformation. The values of the torsion angles of the spermine molecule bound to the pure-spermine form of Z-DNA and also of spermine phosphate hexahydrate (Iitaka & Huse, 1965) are shown in Figure 5, panels A and B. The conformation of spermine bound to the pure-spermine form of Z-DNA resembles a *zig-zag* line, interrupted by a bend near one end of the molecule and a more moderate bend near the other end. The sharper bend is near one of the terminal nitrogens (N1) and results from a negative *synclinal* torsion angle around the C3–C4 bond. The slight bend near the other end of the spermine molecule results from the negative *anticlinal* torsion angle around the C11–C12 bond. Thus the two bends in the spermine molecule occur in bonds that are related by the internal pseudo-2-fold axis of the spermine molecule. As a comparison, the polyamine in the crystal structure of spermine phosphate lies on a crystallographic 2-fold rotation axis. The spermine adopts a fully extended zig-zag chain with antiperiplanar torsions and is almost planar. In the crystal structure of spermine tetrahydrochloride (Giglio

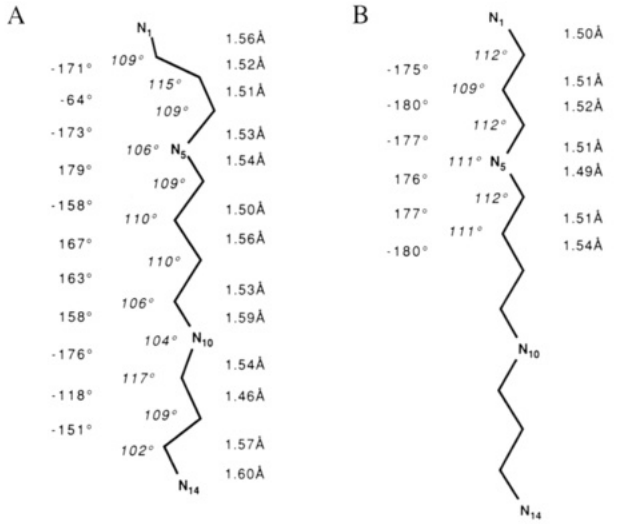

FIGURE 5: (A) Geometry of spermine in the pure-spermine form. (B) Geometry of spermine in the crystal structure of spermine phosphate hexahydrate (Iitaka & Huse, 1965). Bond lengths are on the right; bond angles (italics) and torsion angles are on the left. The spermine molecules are bold, and nitrogen atoms are labeled. The stick drawings are representative of the approximate conformations of spermine. The spermine molecule in the crystal structure of spermine phosphate adopts crystallographic 2-fold symmetry.

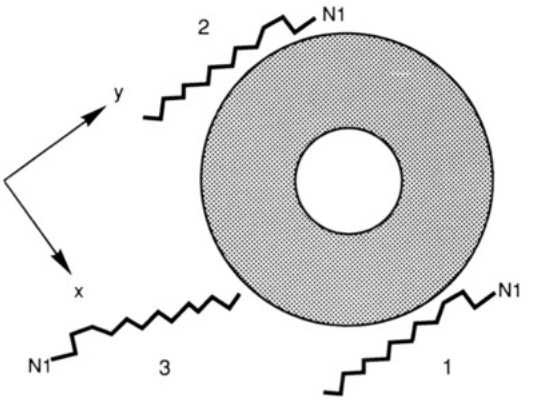

FIGURE 6: Schematic diagram of an axial view of the interactions and relative orientations of a Z-DNA duplex (cylinder stippled in grey) with three symmetry-related spermine molecules. The numbers by which the spermine molecules are referred to in the text are included next to the spermine molecules. To facilitate orientation within the following stereodrawings and to show the symmetry relations among the spermine molecules, the positions of the N1 nitrogens have been labeled and the duplex orientation in the *xy* layer is defined by an axis system.

Table V: DNA–Spermine Interactions[a]

spermine	DNA		
atom (residue 13)	residue	atom	distance (Å)
N1	C(3)	O2P	2.82
N1	G(12)	O2P*	2.77
N1	14	W16	2.96
N5	C(11)	O1P*	2.82
N5	14	W08	2.78
N10	G(8)	N7	2.87
N10	C(9)	O2P**	2.54
N14	G(10)	N7**	3.00
N14	G(10)	O6**	3.03

[a] The residue numbers and symmetry operators are in relation to spermine molecule 1, surrounded by three symmetry-equivalent DNA duplexes. The symmetry operator for atoms with an asterisk is ($x + 1$, y, z) and for those with a double asterisk, it is ($x + 0.5$, $-y + 0.5$, $-z + 1$). Atoms with asterisks belong to the single strand located on the left side of Figure 11, and atoms with a double asterisk belong to the single strand in the background of Figure 11.

et al., 1966), the torsions around bonds N5–C6 and C9–N10 (see the numbering in Figure 5) are in the gauche conformation. The centrosymmetric spermine molecule is therefore bent twice and is characterized by three approximately planar groupings of atoms. Unlike the spermines in the crystal structures of spermine phosphate hexahydrate and spermine tetrahydrochloride, the spermine molecule in the pure-spermine form of Z-DNA does not adopt crystallographic symmetry. The bond lengths and bond angles of spermine in the pure-spermine form of the Z-DNA hexamer are within the expected range, except for the C9–N10 and C13–N14 bonds, which are 0.1 Å longer compared to the values found in the small molecule structure. In addition, the C11–C12 bond is 0.06 Å shorter than the corresponding distance in the small molecule structure.

DNA–Spermine Interactions. Every DNA duplex of the pure-spermine form interacts simultaneously with three spermine molecules, labeled 1, 2, and 3 in Figure 6. In turn, each of these three spermine molecules interacts differently from the other two with a central duplex. However, the three spermine molecules are crystallographically identical; spermine molecules 1 and 2 are related to each other by a translation along the x direction, and spermine molecules 1 and 3 are related by a 2-fold screw axis along the x direction. One Z-DNA duplex plus the three spermine molecules are shown schematically in Figure 6. Figures 7, 8, and 9 illustrate the spermine interactions of the pure-spermine form Z-DNA duplex from three different views. Hydrogen-bond distances are listed in Table V.

Spermine molecule 1 binds to the convex surface (the Z-DNA equivalent of the the major groove) of this Z-DNA duplex. The N10 forms hydrogen bonds to the N7 of residue G(8) (2.87 Å). The spermine molecule spans the complete width of the convex surface (Figure 8) such that the N1 forms a hydrogen bond to the phosphate oxygen O2P of residue C(3) (2.82 Å). There are no other close contacts (<3.3 Å) with this Z-DNA duplex. Spermine 3 also forms two hydrogen bonds to the convex surface of this Z-DNA duplex. These hydrogen bonds link the N14 of spermine molecule 3 to the N7 (3.00 Å) and O6 (3.03 Å) positions of residue G(10). In addition, N10 of this spermine 3 forms a hydrogen bond to a phosphate oxygen (O2P) of residue C(9) (2.54 Å). On the opposite side of the duplex, spermine molecule 2 runs along the rim of the minor groove (Figure 8), forming two hydrogen bonds to the Z-DNA duplex. The first hydrogen bond is from N1 of the spermine molecule to oxygen O2P of residue G(12) (2.77 Å), and the second is from N5 to oxygen O1P of residue C(11) (2.82 Å). At no point does spermine molecule 2 protrude into the groove. In the lower part of the duplex, the spermine molecule is more distant from the backbone which borders one side of the minor groove (Figures 7 and 9). The distances between nitrogen N10 of spermine 2 and the atoms of the phosphate group of residue G(10) are 4.71 Å (P10), 4.90 Å (O1P), and 4.23 Å (O2P). Nitrogen N14 is about equally distant from the phosphates of residues G(8) and C(9). The distances between N14 and the atoms of the former phosphate group are 8.78 Å (P8), 7.47 Å (O1P), and 9.32 Å (O2P), and the distances between N14 and the latter phosphate group are 8.75 Å (P9), 7.48 Å (O1P), and 9.07 Å (O2P).

Figure 10, panels A and B, shows space-filling representations of the Z-DNA–spermine complexes [the views are the same as in Figures 8 (10A) and 9 (10B)]. Figure 10A illustrates how the spermine molecule adheres to the convex surface of the DNA, whereas Figure 10B illustrates the op-

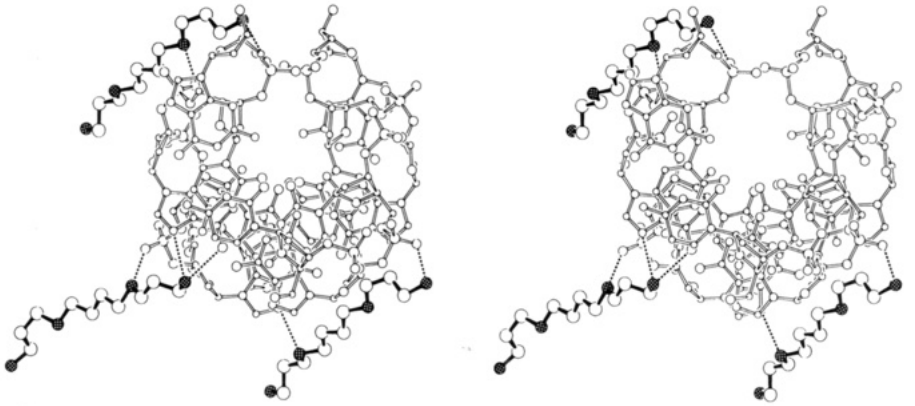

FIGURE 7: ORTEP stereodrawing of the Z-DNA duplex interacting with three symmetry-related spermine molecules, viewed approximately along the helical axis. The DNA is drawn with hollow bonds, and the spermine molecules are drawn with solid bonds. Spermine carbons are drawn as circles with larger radii, spermine nitrogens are stippled, and hydrogen bonds are dashed.

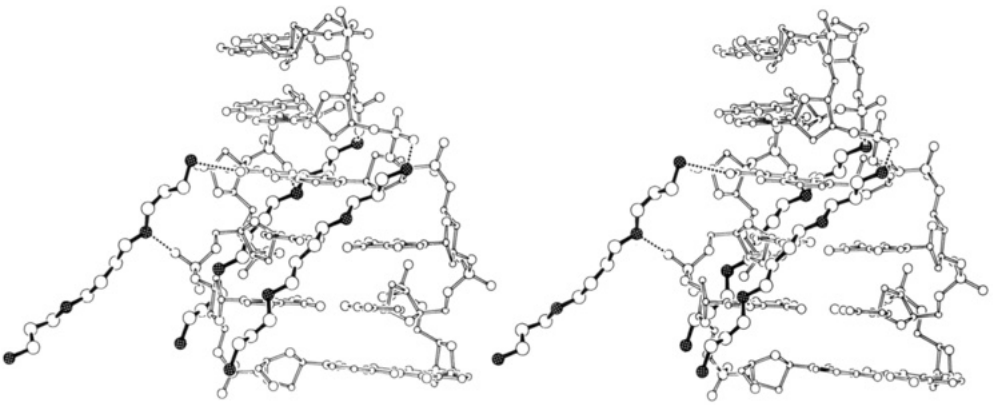

FIGURE 8: ORTEP stereodrawing of the Z-DNA duplex interacting with three symmetry-related spermine molecules, viewed into the convex surface of the DNA (spermine 1 of Figure 5 is in the foreground). The DNA is drawn with hollow bonds, and the spermine molecules are drawn with solid bonds. Spermine carbons are drawn as circles with larger radii, spermine nitrogens are stippled, and hydrogen bonds are dashed.

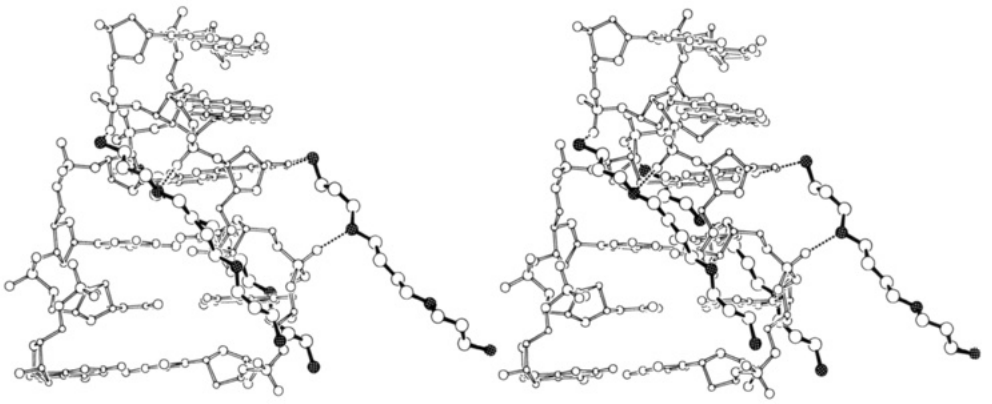

FIGURE 9: ORTEP stereodrawing of the Z-DNA duplex interacting with three symmetry-related spermine molecules, viewed into the minor groove of the DNA (spermine 2 of Figure 5 is in the foreground). The DNA is drawn with hollow bonds, and the spermine molecules are drawn with solid bonds. Spermine carbons are drawn as circles with larger radii, spermine nitrogens are stippled, and hydrogen bonds are dashed.

posite side of the duplex, where spermine molecule 2 follows the phosphate groups along the backbone on the border of the minor groove.

Every spermine molecule of the pure-spermine form interacts simultaneously with three Z-DNA duplexes. Each of the three duplexes surrounding a given spermine molecule interacts differently from the other two. The simultaneous interactions of three duplexes with a single spermine molecule are shown in Figure 11. The interaction distances are given in Table V. It should be noted that these three Z-DNA duplexes are crystallographically identical: Z-DNA duplexes 1 and 2(*) are related to each other by a translation along the *x* direction, and duplexes 1 and 3(**) are related by a 2-fold screw axis along the *x* direction. The N1 forms three hydrogen bonds: two are to phosphate oxygens of different duplexes, O2P of residue C(3) and O2P of residue G*(12), and the third is to water molecule W16(14). The N5 forms two hydrogen bonds: one is to a phosphate oxygen, O1P of residue C*(11), and the second is to water molecule W08(14). The N10 forms two hydrogen bonds: one is to N7 of residue G(8), and the second is to O2P of residue C**(9). The N14 forms two hydrogen bonds: one is to N7, and the other is to O6 of residue G**(10). The N14 is the only nitrogen of the spermine molecule which does not form the maximum number of possible hydrogen bonds. Careful examination of difference electron-density maps in the region around nitrogen N14 did not reveal any

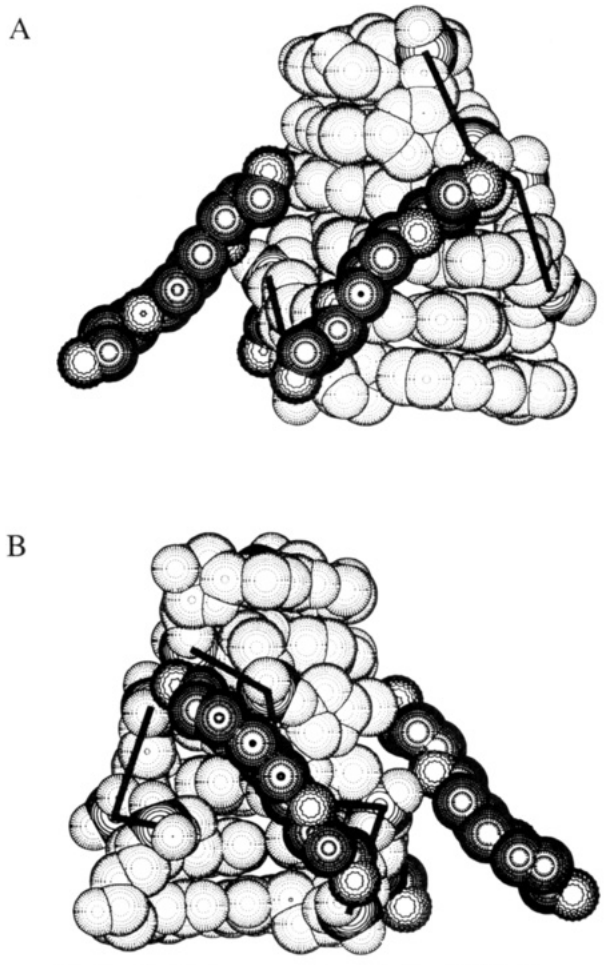

FIGURE 10: Van der Waals representations viewing (A) into the convex surface of the DNA (spermine 1 of Figure 5 is in the foreground) and (B) into the minor groove of the DNA (spermine 2 of Figure 5 is in the foreground). DNA atoms except for phosphorus atoms are dashed, phosphorus atoms are marked with solid circles, and phosphate groups (atoms P, O1P, and O2P) are shaded in grey. Spermine carbons are marked with concentric circles with radial lines, and spermine nitrogens are marked with wavy circles. The DNA backbones are traced with solid lines.

density suggesting the presence of a third ligand.

Data collected at low temperature (−110 °C) reveal a second, possibly disordered, spermine molecule. This second spermine molecule is not observed in the room temperature structure described here. The low-temperature structure and the detailed interactions of the second spermine molecule with the DNA will be discussed in a future publication. From this initial low-temperature data, it was not possible to determine whether there was just one additional spermine molecule or whether the additional sum and difference electron density can be attributed to one and a half spermine molecules. Thus, we cannot answer the question of how the 10 negative charges of the DNA are neutralized in the pure-spermine form crystal. It is possible that there are just two spermine molecules per asymmetric unit, which would require the presence of two sodium ions to fully neutralize the negative charges of the DNA. Alternatively, two spermine molecules (one may be disordered) and one partially occupied spermine position (50%) per asymmetric unit would be sufficient for charge neutralization. NMR investigations in solution showed a complete transition from the B to the Z conformation for the hexamer $[d(m^5CGm^5CGm^5CG)]_2$ with a 2 spermine:1 duplex stoichiometry (Banville et al., 1991). These findings are in accordance with the above low-temperature crystallographic data and suggest the binding of at least two spermine molecules to the left-handed duplex. It is interesting that there is no indication of additional spermine molecules in the room temperature structure. This fact makes it more likely that the additional spermine(s) will also be disordered in the low-temperature structure. However, the degree of disorder at low temperature is much smaller than in the room temperature structure.

Crystal Packing. The volume of the unit cell of the spermine lattice of $[d(CGCGCG)]_2$ is less than that of the magnesium lattice. The unit cell volume of the pure-spermine form (in the spermine lattice) is 24436 Å^3 and is thus 712 Å^3 (3%) less than that of the mixed spermine/magnesium form crystal and is 600 Å^3 (2.5%) less than that of the magnesium form crystal (both of which crystallize in the magnesium lattice). This decrease in the unit cell volume is caused by compression along the helical axis, rather than in the perpendicular to the helical axis. Thus, compared to the magnesium form, the *a* cell constant of the pure-spermine form is longer by around 2.2% and the *b* cell constant is shorter by 0.8%. Table I shows that the average *c* cell constant of the selected magnesium lattices is 44.76 Å. The minimum observed *c* cell constant of the magnesium lattices is 44.38 Å, more than 1.2 Å longer compared to that of the pure-spermine form. In comparison to the pure-spermine form, the *c* cell constant in the mixed spermine/magnesium form is 3.3% longer and that of the magnesium form is 3.8% longer. In comparison to their

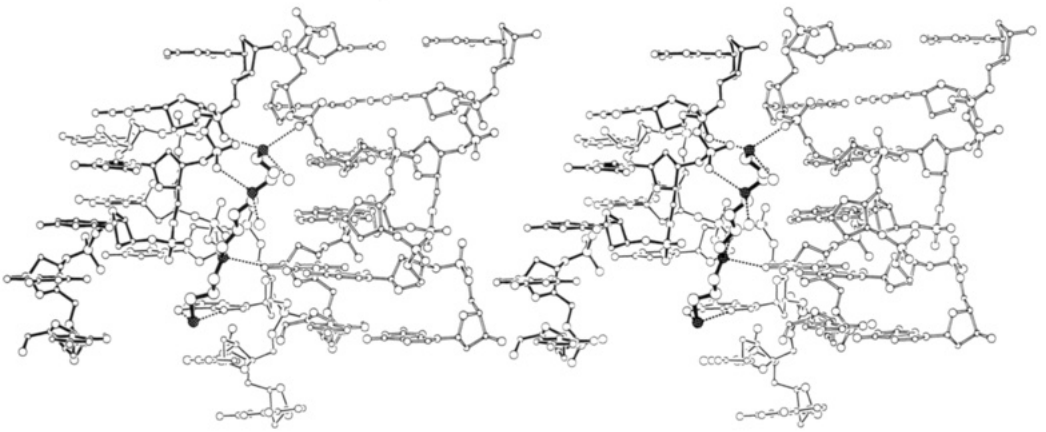

FIGURE 11: ORTEP stereodrawing of a spermine molecule interacting with three Z-DNA duplexes. Spermine bonds are solid, spermine carbons are drawn as circles with larger radii, and spermine nitrogens are stippled. Nitrogen N1 is toward the top of the figure, and nitrogen N14 is toward the bottom. One Z-DNA duplex is drawn with hollow bonds; portions of two others are shown as single strands. One of these is drawn with solid thick bonds and the other with solid thin bonds. Hydrogen bonds are dashed, and oxygen positions of water molecules are drawn as circles with larger radii.

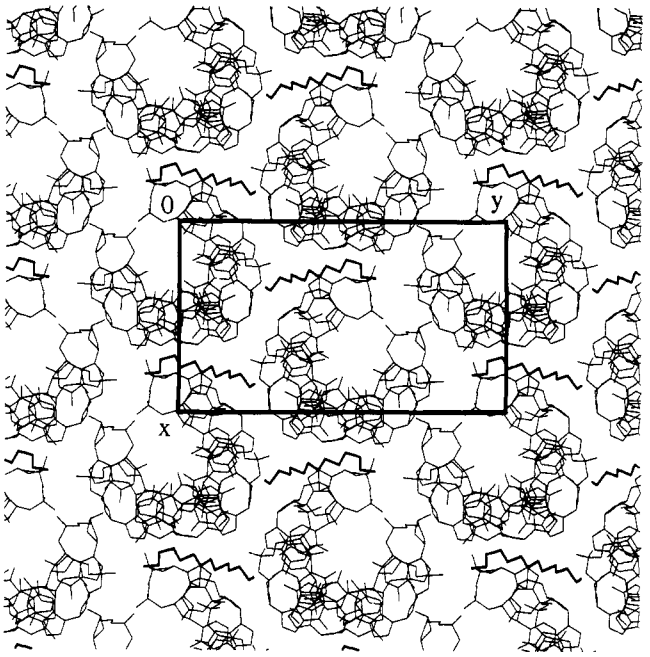

FIGURE 12: Packing arrangement in the crystal lattice of the pure-spermine form, viewed along the *z* direction. The drawing shows an *xy* layer of approximately 20-Å thickness centered around $z = {}^3/_4$. The unit cell is outlined by a heavy line.

orientation in the magnesium lattice, Z-DNA duplexes are rotated around their helical axes (approximately around the *z*-axes) in the spermine lattice. However, due to the cylindrical shape of the duplex, this rotation has only a moderate effect on the *x*- and *y*-axes. The rotation of the duplex, upon shifting from the magnesium lattice to the spermine lattice, conserves the pseudohexagonal arrangement of duplexes (Figure 12). The ratio of *x*-axis to *y*-axis should be close to tan 60° (1.73) in a pseudohexagonal lattice. In the pure-spermine form this ratio is 1.67, in the magnesium form the ratio is 1.72, and in the mixed spermine/magnesium form the ratio is 1.76.

The rotation of the duplex, upon shifting from the magnesium lattice to the spermine lattice, does not significantly alter the stacking interactions between adjacent duplexes in the lattice. In both lattices, the duplexes stack in a 3′–5′ and 5′–3′ manner, forming infinite helices along the *z* direction. The distances between the terminal C3′ atoms of one duplex and the O5′ atoms of the adjacent duplex are 3.39 and 3.49 Å. The mean distance between the terminal base pairs (best planes) of adjacent duplexes is 3.6 Å.

The 3′ termini display pronounced polymorphism. The different interaction schemes of this oxygen in the three structures represent not only differences induced by changing the crystal lattice but also differences in conformation within the same lattice. In the pure-spermine lattice, the O3′ of G(6) (the 3′ terminus of one strand) forms a direct hydrogen bond (2.70 Å) to O1P of residue G(2) of a neighboring duplex (symmetry operator x − 0.5, −y + 1.5, −z + 1). In the magnesium form, this O3′ of G(6) forms a hydrogen bond to O2P of C(9) (2.74 Å). In the mixed spermine/magnesium form, the O3′ does not form direct hydrogen bonds to a neighboring duplex. However, in this case, the O3′ of residue G(6) interacts indirectly with O2P of C(9) via an intervening water molecule W19(16) (2.74 Å). The other terminus is less polymorphic. In both the mixed spermine/magnesium and magnesium forms, the O3′ of residue G(12) forms a hydrogen bond to O1P of residue G(2) from a neighboring duplex. These hydrogen-bond distances are 2.63 Å in the mixed spermine/magnesium form and 2.70 Å in the magnesium form. In contrast, the corresponding O3′ of the pure-spermine form does not interact either directly or indirectly with neighboring duplexes.

C–H···O hydrogen bonds involving the C8 position of guanine appear to be a common structural motif of nucleic acids. In the pure-spermine form of Z-DNA the C8 of residue G(8) of one duplex forms a hydrogen bond to the O2P of residue C(9) of an adjacent duplex. The C8 to O2P distance is 3.18 Å, and the distance between the calculated hydrogen H8 and phosphate oxygen O2P is 2.58 Å (estimating that the C8–H8 distance is 1.0 Å, the sum of the van der Waals radii of an oxygen and a hydrogen atom is about 2.6 Å). The angle at the calculated hydrogen position (angle C8–H8–O2P*) in the pure-spermine form is 119°. In the mixed spermine/magnesium and magnesium forms, there are no definitive examples of C8 hydrogen bonds. However, in the magnesium form, a weak hydrogen bond may link the C8 of residue G(4) to the O5′ of residue G(8) of a neighboring duplex. In this case the C8 to O5′ distance is 3.31 Å, and the angle at the calculated hydrogen position is 150°. We have previously reported that two guanines can interact by forming three hydrogen bonds, one from the O6 of one guanine to the C8 of the other guanine. In this case the calculated hydrogen to acceptor distance was 2.52 Å (Egli et al., 1990).

Hydration. There are 47 ordered water molecules, in addition to a spermine molecule and the hexamer duplex, in the asymmetric unit of the pure-spermine form of $[d(CGCGCG)]_2$. The packing in the pure-spermine form is considerably less dense than that of the mixed spermine/magnesium and magnesium forms. The calculated density of the pure-spermine form is 1.26 g/cm^3, and the ordered water content is 18% (w/w). The calculated density of the magnesium form is 1.37 g/cm^3, and the ordered water content is 29%. The calculated density of the mixed spermine/magnesium form is 1.41 g/cm^3, and the ordered water content is 25%.

All phosphate groups of the pure-spermine form, except for that of residue 4, accept at least one hydrogen bond from a water molecule. The phosphate group of residue G(10) accepts four hydrogen bonds, whereas the phosphate groups of residues C(3), C(5), G(6), C(9), and C(11) each accept three hydrogen bonds. The O2P of residue G(8) accepts two hydrogen bonds, and the O1P of residue G(12) accepts two hydrogen bonds. The O2P of residue G(2) accepts a single hydrogen bond. In the pure-spermine form there are 14 intramolecular DNA–DNA hydrogen bonds mediated by a water molecule (Table VI). In two of these cases, the water molecule links three positions of the DNA such that the DNA forms a tridentate ligand to the water molecule [W05(14) and W02(15), Table VI]. In addition, there are two water-mediated hydrogen bonds linking different duplexes in the lattice. These lattice contacts are mediated by W17(14), which forms hydrogen bonds to both N4 and O2P of residues C(9) of neighboring duplexes, and water W05(15), which forms hydrogen bonds to O1P of residue C(3) and O3′ of residue G(6) of neighboring duplexes. The symmetry operators in the two cases are different (Table VI). In the mixed spermine/magnesium and magnesium forms, such water molecules, connecting two neighboring duplexes, are much more numerous. In the mixed magnesium/spermine form, there are 10 such water molecules, and, in the magnesium form, there are 13 water molecules linking atoms of two neighboring duplexes.

The positions of eight of the water molecules with two or more contacts to the same DNA duplex in the pure-spermine form are very similar either to water positions in both the magnesium form and the mixed spermine/magnesium form

Table VI: Water Molecules with Two and More Contacts to the Same DNA Duplex or Symmetry-Related Duplexes[a]

water	B factor (Å²)	DNA residue and atom	distance (Å)	angle at water (deg)	magnesium form[b] res.	name	dist.	B	mixed magnesium/spermine form[b] res.	name	dist.	B
14 W02	52	G(6) O6	2.87	61	15	W01	3.03	17	13	W04	2.71	9
		G(6) N7	3.06				3.11				3.18	
14 W05	16	C(5) O3′	3.24	93	17	W03	3.28	44	16	W12	3.21	13
		G(6) N2	3.08	43								
		G(6) O2P	3.18	131			2.33				2.72	
14 W07	21	C(5) O2P	2.92	99								
		G(6) O1P	2.73									
14 W13	44	C(5) O2	3.10	80	18	W04	2.99	19				
		C(9) O2	3.21				3.03					
14 W16	14	C(5) O1P	2.77	122								
		G(6) O1′	3.26									
14 W17[1]	22	C(9) N4	3.08	126								
		C(9) O2P*	3.31									
14 W18	32	C(3) O2	3.20	70	17	W19	2.92	18	16	W02	3.01	24
		C(9) O2	3.12				3.13				3.05	
14 W25	12	G(10) N2	3.22	127	17	W11	3.11	13	17	W11	3.10	10
		C(11) O1P	2.94				2.94				2.97	
15 W02	20	C(11) O3′	3.33	90	18	W21	3.36	42				
		G(12) N2	3.08	44								
		G(12) O1P	3.11	130			3.26					
15 W05[1]	24	C(3) O1P	2.55	97								
		G(6) O3′**	2.90									
15 W06	17	G(2) N2	3.15	117	18	W22	3.10	12	16	W24	3.12	8
		C(3) O1P	3.29				2.99				2.81	
15 W09	31	C(3) O2	2.94	99	18	W18	3.01	31	17	W02	3.03	27
		C(11) O2	2.69				2.90				3.15	
15 W10	24	C(1) O2	3.16	72								
		C(11) O2	2.82									
15 W22	54	C(9) O1P	3.33	99								
		G(10) O2P	2.93									

[a] Water molecules with contacts to two different DNA duplexes are designated with a superscript 1, and symmetry-generated atoms are designated with asterisks. For water molecules with three contacts to the DNA, the three given angles at the water molecule are the angle formed by atom1, a water molecule, and atom2, the angle between atom1, a water molecule, and atom3, and the angle between atom2, a water molecule, and atom3. The columns headed by "magnesium form" and "mixed magnesium/spermine form", respectively, list the water molecules and their residue numbers in the other two Z forms with DNA contacts which correspond to the ones present in the structure described here. In addition, the hydrogen-bond distances (middle) and temperature factors of the water molecules (right) are listed. [b] Residue, name, distance, and *B* value.

or to a water position in at least one of those two forms (Table VI). Most of the conserved positions are water molecules with contacts to two O2 oxygens of different bases in the minor groove (3). The hydrogen bonds between water W25(14) and N2 of residue G(10) and O1P of residue C(11) are also observed in the magnesium and mixed spermine/magnesium forms, and the geometries of those hydrogen bonds in the three structures are almost identical. Furthermore, the *B* factors of these water molecules are very similar for the three structures. In general, the *B* factors of water molecules with conserved hydrogen bonds between the three forms are quite similar (Table VI). Differences in *B* factors of water molecules in the pure-spermine form in comparison to the mixed spermine/magnesium or magnesium forms can be attributed to interactions of those water molecules with magnesium ions in the mixed spermine/magnesium and magnesium forms.

In the pure-spermine form there are 10 water molecules which make four hydrogen bonds. Of these 10 water molecules, three are in the proximity of a fifth ligand. There is often a difficulty in assigning sodium ions in hydrated crystals. In each of the three cases above, the distance to the fifth ligand is slightly longer than expected for a sodium–water interaction (distance ca. 2.5 Å). A careful examination of electron sum- and difference-density maps did not reveal density indicating misplaced or missing atoms. Water molecule W14(14) is coordinated to four water molecules (2.53, 2.86, 3.03, and 3.06 Å). A fifth potential ligand is O1P of residue G(10) (3.37 Å). Water molecule W01(15) is coordinated to three water molecules (2.93, 3.02, and 3.03 Å) and also to O1P of residue G(10) (2.96 Å). A fifth potential ligand is an additional water molecule (3.17 Å). Water molecule W10(15) forms hydrogen bonds to the O2 positions of residues C(1) and C(11) (2.82 and 3.16 Å, Table VI) and to two water molecules (3.15 and 3.26 Å). A fifth potential ligand is another water molecule (3.24 Å). The inability to visualize two positively charged sodium ions which are required to fully neutralize the DNA could be explained by solvent disorder. As described above, the backbone in the region surrounding P9 is disordered, partially occupying both the ZI and the ZII conformation. Previously, it was suggested that the ZII conformation is specifically stabilized by ions (Wang et al., 1981). Thus, it is likely that the ion positions in the region surrounding P9 would be partially occupied.

Molecular Motion. The isotropic temperature factors (*B* factors) describe the mobility of atoms and molecules within a crystal. As previously described, the temperature factors associated with bases are slightly lower than those associated with the sugar–phosphodiester backbone (Gessner et al., 1989; Egli et al., 1990). The phosphate groups display the highest thermal motion in crystal structures of DNA, as might be

anticipated. The average *B* factors for bases and sugars in the pure-spermine form are generally between 6 and 10 Å^2 (room temperature measurement). The atoms of phosphate groups (O3′, O5′, P, O1P, and O2P) in the pure-spermine form have temperature factors between 8 and 16 Å^2. The phosphate group of residue C(11) possesses the lowest *B* factors (P11, 7.7 Å^2; O1P, 9.3 Å^2; O2P, 9.41 Å^2). There is no clear relationship within the pure-spermine form duplex between thermal motion and position within the duplex. The magnitudes of the molecular motion at the two ends of the duplex are comparable. Furthermore, the thermal motion of the terminal base pairs is not greater than within the middle of the duplex, as would be expected in solution. Similar patterns have been described previously for the magnesium form (Gessner et al., 1989).

The disorder of the backbone in the region around phosphate P9 is indicated by higher *B* factors of that phosphate group. The *B* factors of phosphorus P9 (15.1 Å^2) and oxygens O1P (16.0 Å^2) and O2P (15.9 Å^2) are the highest among phosphate groups. The *B* factors of O3′ of residue G(8) (11.4 Å^2) and O5′ of residue C(9) (11.3 Å^2) are higher than those of the corresponding atoms in the other deoxyriboses, and their values are comparable to those of the terminal O3′ and O5′ oxygens. Although the *B* factors of the phosphate group of residue C(9) are higher than those of the neighboring residues, the deoxyribose atoms (with exception of O3′ and O5′, which are attached to phosphate P9) of residues G(8) and C(9) display *B* factors which are comparable to those of other residues.

One end of the spermine molecule within the pure-spermine form of Z-DNA appears to be more tightly constrained than the other end. The *B* factors of atoms at one end of the spermine molecule are lower than those of atoms at the other end. The *B* factors of atoms N1 to C6 are all between 9 and 10 Å^2, whereas the *B* factors of atoms C7 to N14 are between 12 Å^2 for atom C7 and 20 Å^2 for atom N14, with continuously rising *B* factors when moving along the spermine chain from atom C7 to ammonium nitrogen N14. This pattern is somewhat surprising considering the interactions of the nitrogen atoms of the spermine molecule. Although both N1 and N5 are involved in the maximum of their possible interactions (unlike N14 in the other moiety of the spermine molecule), two of the contacts are to water molecules, which are usually associated with much higher thermal motion than DNA atoms.

Discussion

The mixed spermine/magnesium and magnesium forms of $[d(CGCGCG)]_2$ previously have been the focus of detailed analysis. In addition, over a dozen related Z-DNA hexamers have been crystallized and their structures solved. The complete series, with the exception of the pure-spermine form described here, is isomorphous with respect to the DNA orientation and position.

The structure of the mixed spermine/magnesium form, obtained from a solution containing both magnesium and spermine, was determined at 0.9-Å resolution and refined to an *R* factor of 14% (Wang et al., 1979, 1981). In a further analysis of this structure, the atomic positions were refined anisotropically, resulting in an *R* factor of 12.9% (Holbrook et al., 1986). In the mixed spermine/magnesium form, each DNA hexamer duplex is complexed by two spermine molecules and one partially hydrated magnesium ion. The structure of the magnesium form, obtained from a solution containing magnesium and buffer as the only cations, was determined at 1.0-Å resolution and refined to an *R* factor of 17.5% (Gessner et al., 1989). In the magnesium form, each DNA hexamer duplex is complexed by four magnesium ions, three of them fully hydrated and one of them partially hydrated.

In both the mixed spermine/magnesium form and the magnesium form, the magnesium ions are not evenly distributed around the DNA but are arranged in clusters. In the magnesium form there are two water molecules that each simultaneously coordinate two magnesium ions. These two magnesium ions are linked to a third through their second hydration shells. The ionic interactions in the magnesium form generally have an analogous counterpart in the mixed spermine/magnesium form. The lone magnesium ion observed in the mixed spermine/magnesium form is located at the same position as one of the ions in the magnesium form. On the basis of these similarities, it was suggested that the binding sites of positively charged counterions are determined predominantly by the structure and conformation of the DNA and not by the nature of the ions (Gessner et al., 1989). However, differences in the packing arrangements of spermine–Z-DNA and magnesium–Z-DNA suggest that packaging of DNA in vivo would depend on the structure(s) of the cation(s).

In the mixed spermine/magnesium form, one of the spermine molecules forms a series of hydrogen bonds to the convex surfaces of two different (but symmetry-related) Z-DNA duplexes. Each of the four amino groups of this spermine molecule forms at least one hydrogen bond to the DNA. These hydrogen bonds are to O6 and N7 positions of guanines. The second spermine molecule interacts simultaneously with three different (but symmetry-related) duplexes. Compared to the first spermine, it forms half as many hydrogen bonds to DNA bases but twice as many to phosphate oxygens. The high temperature factors as well as the distorted geometry of the second spermine suggest only partial occupancy within the crystal.

The pure-spermine form of $[d(CGCGCG)]_2$ is unique among Z-DNA crystals obtained thus far. This high-resolution structure constitutes the first crystallographic analysis of a Z-DNA fragment in the absence of inorganic polyvalent cations. The orientation and position of the hexamer duplex differ from all previously described Z-DNA crystal structures. In experiments to cocrystallize the DNA fragment $[d(CGCGCG)]_2$ with various polyamines, we avoided the crystallization within the magnesium lattice by excluding magnesium ions and other polyvalent ions from the crystallization solutions.

Briefly summarized, earlier polyamine Z-DNA complexes have exhibited the following characteristics of polyamine–DNA interaction [reviewed in Tomita et al. (1989) and Williams et al. (1991)]: (a) on the convex surface, amino groups tend to form hydrogen bonds to the N7 positions of guanines, (b) a subset of these simultaneously form hydrogen bonds to O6 positions of the same guanine, (c) amino groups commonly form hydrogen bonds with phosphate oxygens, (d) terminal amino groups are located near the minor groove of Z-DNA or actually penetrate it, (e) the conformation of the polyamine molecule is not always extended (all-trans or zig-zag form), and (f) polyamines do not interact with a single DNA molecule but interact simultaneously with two or three DNA molecules.

The interactions between the spermine molecule and the DNA in the pure-spermine form follow the above pattern. With a single exception, the hydrogen-bonding capacity of the spermine molecule to form a total of 10 hydrogen bonds is fully realized in the crystal described here. The terminal ammonium nitrogens of a spermine molecule can form three hydrogen

bonds, and the internal imino nitrogens can each form two. The spermine molecule in the crystal forms a total of nine hydrogen bonds, three to one duplex, two each to two others, and two to water molecules. One of the terminal nitrogen atoms (N14) forms hydrogen bonds to O6 and N7 of a guanine. One of the two hydrogen bonds formed by the neighboring nitrogen (N10) is to a guanine N7 of a different, symmetry-related, duplex. This is somewhat similar to the observed interactions between one of the spermines and the DNA in the mixed spermine/magnesium form. There, one of the central imino nitrogen atoms forms hydrogen bonds to both O6 and N7 of guanine, and the neighboring terminal nitrogen forms a hydrogen bond to the guanine N7 in the adjacent base pair of the same duplex. The other hydrogen bonds between the spermine molecule and the DNA in the pure-spermine form are to phosphate oxygens (4) and to water molecules. Thus, the spermine molecule in the pure-spermine form interacts with the DNA via hydrogen bonds and charge–charge interactions. The spermine molecule does not form any hydrophobic contacts with the DNA. This is in contrast to the interactions between spermine and A-DNA (Jain et al., 1989) and B-DNA anthracycline complexes, but consistent with the results from other Z-DNA crystal structures [reviewed in Williams et al. (1991)]. Nevertheless, hydrophobic interactions are probably not unimportant in the spermine Z-DNA complex and might play a role in the condensation of DNA into compact structures. In the mixed spermine/magnesium form the methylene groups of adjacent spermine molecules provide a significant contribution to the stability of the spermine–Z-DNA complex. In the pure-spermine form, there are no hydrophobic interactions between spermine molecules. The arrangement of a second spermine molecule found in a preliminary low-temperature study may change this picture somewhat, leading to the formation of hydrophobic contacts between the spermines.

Compared to earlier forms of Z-DNA, the DNA in the pure-spermine form is compressed along the helical axis. A second alteration of the helix geometry of the pure-spermine form is the general shift of base pairs away from the helical axis into the major groove (x displacement), although the extent of x displacement differs significantly among base pairs. The changes resulting from the increased x displacement and the indirect effects of this on stacking interactions might be responsible for the compression along the helical axis. It is possible that the smaller overlap between base pairs reduces steric hindrance and allows a more compact arrangement of the stacks along the helical axis. The helical rise per base pair in the pure-spermine form is more regular than that of the magnesium form or the mixed spermine/magnesium form. The values for the helical rise in the pure-spermine form vary between 3.63 and 3.70 Å, whereas the values in the magnesium form vary between 3.65 and 4.02 Å and those of the mixed spermine/magnesium form vary between 3.37 and 4.33 Å.

The width of the minor groove of the pure-spermine form of Z-DNA is less than that of the magnesium or mixed magnesium/spermine forms. This reduction in the width of the minor groove may be attributable to the location of an additional spermine molecule within the minor groove. This second spermine molecule is not observed in the room temperature structure described here. However, preliminary data collected at low temperature clearly reveal at least a second, possibly disordered, spermine molecule.

The ZI conformation of Z-DNA, with the phosphate group directed away from the convex surface, is more commonly observed than the ZII conformation, with the phosphate group directed in toward the convex surface (Wang et al., 1981; Gessner et al., 1989). In both the mixed spermine/magnesium and magnesium forms, the backbone in the region around the phosphate of residue C(5) adopts the ZII conformation. In contrast, in the pure-spermine form the backbone in the same region adopts the ZI conformation. In both the mixed spermine/magnesium and magnesium forms, a magnesium ion is bound to the N7 of residue G(6). A water molecule coordinated to this magnesium ion forms a hydrogen bond to a phosphate oxygen of residue C(5), appearing to stabilize the ZII conformation. The ZI rather than ZII conformation region around the phosphate of residue C(5) in the pure-spermine form would appear to support a previous suggestion that magnesium ions stabilize the ZII conformation. However, the pure-spermine form demonstrates that divalent cations are not necessarily required for conversion of ZI to ZII. In the pure-spermine form, the backbone around phosphate P9 appears to partially occupy both the ZI and ZII conformations. It appears that greater than 50% of the population of the Z-DNA duplexes in the crystal adopts the ZI conformation, but a substantial fraction also adopts the ZII conformation. Thus, in the absence of divalent ions, a significant fraction of the population adopts the ZII conformation, indicating that the stability of the ZII conformation can approach that of the ZI conformation, even in the absence of polyvalent cations. The polymorphic nature of the backbone in the crystalline state suggests that in solution Z-DNA would flip between nearly isoenergetic ZI and ZII conformations. It is not clear whether the partial occupancy of the ZII conformation is associated with a bound sodium ion, also partially occupied, or whether packing forces facilitate a high degree of conformational freedom at this site.

The patterns of hydrogen bonding between DNA and bound water are generally conserved in the two different lattices (Table VI). This invariance indicates that solution hydration is not highly perturbed by the lattice. Thus, it is likely that the patterns of hydration observed crystallographically are similar to those in solution. In certain cases a water molecule forms three hydrogen bonds to the DNA in the pure-spermine form, but the corresponding water molecules in the other forms make only two hydrogen bonds to the DNA. However, in these cases there is generally a second water molecule in the mixed spermine/magnesium or magnesium forms which forms a hydrogen bond to the DNA, which compensates for the lack of a third hydrogen bond by the first water molecule. The patterns of hydrogen bonding are very similar in the minor groove of the three forms of Z-DNA. In the minor groove, water molecules link the O2 atoms of adjacent cytosines, forming a partially buried spine of hydration. Thus, in the minor groove water molecules connect the O2 of C(1) to the O2 of C(11), the O2 of C(11) to the O2 of C(3), the O2 of C(3) to the O2 of C(9), and the O2 of C(9) to the O2 of C(5), etc. This hydrogen-bonding scheme is preserved throughout the series of Z-DNA crystal structures, in most cases with very similar geometry of the hydrogen bonds (Table VI). There are four water molecules in the room temperature structure of the pure-spermine form which are situated in regions of positive electron sum and difference density in a preliminary low-temperature structure, attributed to the second spermine molecule. These four water molecules are W02(14), W19(14), W08(15), and W10(15). Whereas W02(14) and W10(15) are water molecules whose positions are conserved between pure-spermine, magnesium, and mixed spermine/magnesium forms, it is possible that the two other water molecules should rather be interpreted as peaks in the electron-density maps due

to a second disordered spermine. However, neither position showed abnormal behavior during refinement, and their *B* factors are within the range expected for a room temperature structure. In some cases, the patterns of hydration of three forms of Z-DNA are similar in a manner not apparent in Table VI. Only distances of less than 3.4 Å were included in the hydrogen-bonding schemes. In some cases, positions of water molecules may have been conserved between different forms, but the donor–acceptor distances were longer than the arbitrarily used threshold and thus these contacts do not show up as conserved hydrogen bonds in Table VI.

To neutralize the 10 negative charges of the phosphate groups of the Z-DNA duplex requires two positive charges in addition to the four positive charges of each spermine molecule. The only source of positive charge in the crystallization reservoir other than spermine was sodium (the buffer was 20 mM sodium cacodylate). It is possible that two of the atoms which were refined as oxygens of water molecules were actually sodium ions. In principle, it is possible to distinguish a sodium from a water molecule by differences in coordination geometry. Water molecules tend to assume four-coordinate tetrahedral geometry, and sodium ions tend to assume six-coordinate octahedral geometry. However, none of the water molecules found in the pure-spermine form crystal are six coordinate, and it was not possible to unambiguously assign any electron-density peaks as sodium ions.

ACKNOWLEDGMENTS

We thank Professor Jack D. Dunitz and Drs. Daniel Bancroft and Reinhard Gessner for helpful suggestions.

REFERENCES

Basu, H. S., Feuerstein, B. G., Zarling, D. A., Shafer, R. H., & Marton, L. J. (1988) *J. Biomol. Struct. Dyn. 6*, 299–309.

Banville, D. L., Feuerstein, B. G., & Shafer, R. H. (1991) *J. Mol. Biol. 219*, 585–590.

Behe, M. J., & Felsenfeld, G. (1981) *Proc. Natl. Acad. Sci. U.S.A. 78*, 1619–1623.

Bloomfield, V. A., & Wilson, R. W. (1981) in *Polyamines in Biology and Medicine* (Morris, D. R., & Marton, L. J., Eds.) pp 183–206, Marcel Dekker, New York.

Chen, H. H., Behe, M. J., & Rau, D. C. (1984) *Nucleic Acids Res. 12*, 2381–2389.

Chattoraj, D. K., Gosule, L. C., & Schellman, J. A. (1978) *J. Mol. Biol. 121*, 327–337.

Chevrier, B., Dock, A. C., Hartman, B., Leng, M., Moras, D., Thuong, M. T., & Westhof, E. (1986) *J. Mol. Biol. 188*, 707–719.

Dickerson, R. E., et al. (1989) *Nucleic Acids Res. 17*, 1797–1803.

Egli, M., Gessner, R. V., Williams, L. D., Quigley, G. J., van der Marel, G. A., van Boom, J. H., Rich, A., & Frederick, C. A. (1990) *Proc. Natl. Acad. Sci. U.S.A. 87*, 3235–3239.

Egli, M., Williams, L. D., Frederick, C. A., & Rich, A. (1991) *Biochemistry 30*, 1364–1372.

Feuerstein, B. G., Williams, L. D., Basu, H. S., & Marton, L. J. (1991) *J. Cell. Biochem. 46*, 37–47.

Fujii, S., Wang, A. H.-J., van der Marel, G. A., van Boom, J. H., & Rich, A. (1982) *Nucleic Acids Res. 10*, 7879–7892.

Gessner, R. V., Quigley, G. J., Wang, A. H.-J., van der Marel, G. A., van Boom, J. H., & Rich, A. (1985) *Biochemistry 24*, 237–240.

Gessner, R. V., Frederick, C. A., Quigley, G. J., Rich, A., & Wang, A. H.-J. (1989) *J. Biol. Chem. 264*, 7921–7935.

Giglio, E., Liquori, A. M., Puliti, R., & Ripamonti, A. (1966) *Acta Crystallogr. 20*, 652–659.

Gosule, L. C., & Schellman, J. A. (1978) *J. Mol. Biol. 121*, 311–326.

Hendrickson, W. A., & Konnert, J. H. (1981) in *Biomolecular Structure, Conformation, Function and Evolution* (Srinivasan, R., Ed.) pp 43–57, Pergamon, Oxford.

Ho, P. S., Frederick, C. A., Saal, D., Wang, A. H.-J., & Rich, A. (1987) *J. Biomol. Struct. Dyn. 4*, 521–534.

Holbrook, S. R., Wang. A. H.-J., Rich, A., & Kim, S. H. (1985) *J. Mol. Biol. 187*, 429–440.

Iitaka, Y., & Huse, Y. (1965) *Acta Crystallogr. 18*, 110–121.

Jain, S., Zon, G., & Sundaralingam, M. (1989) *Biochemistry 28*, 2360–2364.

Jones, T. A. (1978) *J. Appl. Crystallogr. 11*, 268–272.

Klyne, W., & Prelog, V. (1960) *Experientia 16*, 521–523.

Mandel, M. (1962) *J. Mol. Biol. 5*, 435–441.

Möller, A., Nordheim, A., Kozlowski, S. A., Patel, D. J., & Rich, A. (1984) *Biochemistry 23*, 54–62.

Morris, D. R. (1981) in *Polyamines in Biology and Medicine* (Morris, D. R., & Marton, L. J., Eds.) pp 223–242, Marcel Dekker, New York.

North, A. C. T., Phillips, D., & Matthews, F. S. (1968) *Acta Crystallogr. A24*, 351–359.

Pegg, A. E., & McCann, P. P. (1982) *Am. J. Physiol. 243*, C212–C221.

Peck, L. J., Nordheim, A., Rich, A., & Wang, J. C. (1982) *Proc. Natl. Acad. Sci. U.S.A. 79*, 4560–4564.

Pohl, F. M., & Jovin, T. (1972) *J. Mol. Biol. 67*, 375–396.

Quigley, G. J., Teeter, M. M., & Rich, A. (1978) *Proc. Natl. Acad. Sci. U.S.A. 75*, 64–68.

Rabinovich, D., & Shakked, Z. (1984) *Acta Crystallogr. A40*, 195–200.

Rao, M. V. R., Atreyi, M., & Saxena, S. (1990) *Biopolymers 29*, 1495–1497.

Rich, A., Nordheim, A., & Wang, A. H.-J. (1984) *Annu. Rev. Biochem. 53*, 791–846.

Sen, D., & Crothers, D. M. (1986) *Biochemistry 25*, 1495–1503.

Singleton, C. K., Klysik, J., Stirdivant, S. M., & Wells, R. D. (1982) *Nature (London) 299*, 312–316.

Tabor, C. W., & Tabor, H. (1984) *Annu. Rev. Biochem. 53*, 749–790.

Tabor, H. (1962) *Biochemistry 1*, 496–501.

Thomas, T. J., & Bloomfield, V. A. (1984) *Biopolymers 23*, 1295–1306.

Tomita, K., Hakoshima, T., Inubushi, K., Kunisawa, S., Ohishi, H., van der Marel, G. A., van Boom, J. H., Wang, A. H.-J., & Rich, A. (1989) *J. Mol. Graphics 7*, 71–75.

Wang, A. H-J., Quigley, G. J., Kolpak, F. J., Crawford, J. L., van Boom, J. H., van der Marel, G. A., & Rich, A. (1979) *Nature (London) 282*, 680–686.

Wang, A. H.-J., Quigley, G. J., Kolpak, F. J., van der Marel, G. A., van Boom, J. H., & Rich, A. (1981) *Science 211*, 171–176.

Westhof, E., Prange, T., Chevrier, B., & Moras, D. (1985) *Biochimie 67*, 811–817.

Widom, J., & Baldwin, R. L. (1980) *J. Mol. Biol. 144*, 431–453.

Williams, L. D., Frederick, C. A., Gessner, R. V., & Rich, A. (1991) in *Molecular Conformation and Biological Interaction* (Ramaseshan, S., & Balaram, P., Eds.) Bangalore, India.

Wilson, R. W., & Bloomfield, V. A. (1979) *Biochemistry 18*, 2192–2196.